Binding of human α-thrombin to platelet GpIb: energetics and functional effects

Raimondo de CRISTOFARO[1], Erica de CANDIA, Giovanni CROCE, Roberta MOROSETTI and Raffaele LANDOLFI

Haemostasis Research Centre, Department of Internal Medicine, Catholic University of Rome, 00168 Rome, Italy

Thrombin interaction with platelet glycocalicin (GC), the 140 kDa extracytoplasmic fragment of the membrane glycoprotein Ib, was investigated by using a solid-phase assay. Thrombin bound to GC-coated polystyrene wells was detected by measuring the hydrolysis of a chromogenic substrate. The monoclonal antibody LJ-Ib10, which specifically binds to the thrombin-binding site of GC, could displace thrombin from immobilized GC, whereas the monoclonal antibody LJ-Ib1, which interacts with the von Willebrand factor-binding domain of GC, did not affect thrombin binding to GC. Competitive inhibition of thrombin binding to immobilized GC was also observed using GC in solution or ligands that bind to the thrombin heparin-binding site, such as heparin and prothrombin fragment 2. Furthermore functional experiments demonstrated that GC binding to thrombin competes with heparin for thrombin inactivation by the antithrombin III–heparin complex as well. Thrombin–GC interaction was also studied as a function of temperature over the range 4–37 °C. A large negative heat capacity change (ΔC_p), of -4.14 ± 0.8 kJ·mol^{-1}·K^{-1}, was demonstrated to dominate the thermodynamics of thrombin–GC complex-formation. Finally it was demonstrated that GC binding to thrombin can allosterically decrease the enzyme affinity for hirudin via a simultaneous decrease in association rate and increase in the dissociation velocity of the enzyme–inhibitor adduct. Together these observations indicate the GC binding to the heparin-binding domain of thrombin is largely driven by a hydrophobic effect and that such interaction can protect the enzyme from inhibition by the heparin–anti-thrombin III complex.

INTRODUCTION

Platelet glycoprotein Ib (GpIb) is the major glycoprotein on the platelet surface and plays an essential role in haemostasis, being involved in von Willebrand factor binding, which regulates the early adhesion of platelets to exposed subendothelium [1]. In addition, GpIb has a high-affinity thrombin-binding site, which may play an important role in thrombin-induced platelet activation [1].

GpIb belongs to the 'leucine-rich repeat' family of proteins [2]. It is a 150 kDa transmembrane glycoprotein and contains a 27 kDa β-subunit connected via a disulphide bond to the α-subunit, bearing the von Willebrand factor- and thrombin-binding sites [3]. The thrombin-binding site of GpIbα maps to a region on the C-terminal side of the leucine-rich repeat domain (residues Cys-209–Asp-287) [4]. Glycocalicin (GC), the 140 kDa extracytoplasmic portion of GpIbα that bears the von Willebrand- and thrombin-binding sites of GpIb, can be produced by the activity on GpIb of proteases such as endogenous calpain [1]. The involvement of the heparin-binding site (HBS) of thrombin in GpIb interaction has recently been demonstrated [5].

In the present study thrombin–GC interaction was studied by a novel solid-phase method, using the wheat-germ agglutinin from *Triticum vulgaris* as the coupling molecule to the solid phase. This approach allowed us to provide a thermodynamic framework for binding and to study the linkage with other macromolecular ligands that bind to the thrombin HBS. Finally, the functional effect of GC binding to the thrombin HBS on the formation of the thrombin–heparin–anti-thrombin III (ATIII) complex was also investigated.

EXPERIMENTAL

Materials

Human α-thrombin was purified and characterized as previously reported [6]. Purified human ATIII (lot HATIII 540AL) and high-molecular-mass heparin (lot HF2025; molecular mass 16 kDa) were purchased from Enzyme Research Laboratories Inc. The molecular mass of this heparin form was confirmed by HPLC analysis performed using a Bio-Silect SEC 250-5 gel-filtration column (Bio-Rad) fitted to a liquid chromatograph (Perkin-Elmer; series 10). Purified heparin oligosaccharides of known molecular mass, from Enzyme Research, were used to construct the reference cure. Heparin was detected at 205 nm. It was then further purified by affinity chromatography using an anti-thrombin column [7]. ATIII showed a single band on SDS/4–20 % polyacrylamide gels with an apparent molecular mass of 58 kDa. The ATIII concentration was calculated spectrophotometrically, using an absorption coefficient ϵ_{280} (1 %) of 6.5 [8]. The chromogenic substrate D-Phe-Pipecolyl-Arg-*p*-nitroanilide (S2238) was from Chromogenix (Molndal, Sweden). Purified wheat-germ lectin, purified human prothrombin and recombinant hirudin variant 2, rHV2K47, were purchased from Sigma (St. Louis, MO, U.S.A.). BSA (fatty acid-free) was from Boehringer-Mannheim Italia SpA (Milan, Italy). The purified anti-GC monoclonal antibodies (mAbs) LJ-Ib10 and LJIb1 were kindly provided by Dr. L. De Marco (Centro Riferimento Oncologico di Aviano, Italy).

Purification of GC

GC was purified as detailed previously using fresh/outdated platelet concentrates [5]. Briefly, after affinity chromatography of

Abbreviations used: GC, glycocalicin; GpIb, glycoprotein Ib; HBS, heparin-binding site; ATIII, anti-thrombin III; S2238, D-Phe-Pipecolyl-Arg-*p*-nitroanilide; mAb, monoclonal antibody; F2, fragment 2; FRS, fibrinogen-recognition site.

[1] To whom correspondence should be addressed.

3 M KCl platelet extract on a wheat-germ lectin–agarose gel, the material eluted was further purified by anion-exchange FPLC, using a high-load Q-Sepharose column (Pharmacia-LKB, Uppsala, Sweden) equilibrated with 20 mM Tris/HCl, pH 7.60 (eluent A). Eluent B was 0.7 M NaCl in eluent A. The gradient was 0–100 % eluent B over 60 min, followed by 10 min with 100 % eluent B. GC was eluted at 100 % eluent B. SDS/PAGE and silver staining confirmed that the purified material was pure, with an apparent molecular mass of 140 kDa. Measurement of GC molecular mass was also carried out by a gel-filtration method, using bovine thyroglobulin, bovine IgG, chicken ovalbumin and equine myoglobin as protein standards. These proteins were chromatographed on a Bio-Rad Bio-Silect SEC 250-5 column (300 mm × 7.8 mm). The column was equilibrated with 0.1 M sodium phosphate buffer/0.15 M NaCl, pH 6.8, at a flow rate of 1 ml/min. Purified GC was eluted slightly ahead of thyroglobulin (molecular mass 670 kDa). The overestimation of the molecular mass of GC by gel filtration was previously demonstrated to be caused by the high asymmetry of the GC molecule [9]. The apparent Stokes radius of purified GC was found to be 8 ± 0.3 nm (80 ± 3 Å), in excellent agreement with the previously reported value of 7.8 nm [9].

Purification of prothrombin fragment 2 (F2)

Human prothrombin (9 mg/ml) was dissolved in 10 mM Tris/HCl, pH 7.8, containing 0.15 M NaCl and 0.1 % PEG 6000, at 37 °C and activated by ecarin (50 units/ml final concentration). After 1 h of incubation, prothrombin F2 was separated and quantified by anion-exchange FPLC at room temperature with a Pharmacia–LKB FPLC chromatograph using a high-load Mono Q HR 10/10 column. The gradient applied was 0–0.5 M NaCl in 20 mM Tris/HCl, pH 7.6, for 1 h at a flow rate of 3 ml/min. F2 was the last peak to be eluted. SDS/PAGE under reducing conditions showed that the apparent molecular mass of purified F2 was 12.5 kDa. F2 concentration was calculated spectrophotometrically using a specific absorption coefficient at 280 nm of 0.95 $ml \cdot mg^{-1} \cdot cm^{-1}$, according to its sequence [10] and the method of Pace and co-workers [11]. Purified F2 was stored at −80 °C until use.

Solid-phase experiments on thrombin–GC interaction

The experiments were designed as 'sandwich' assays, whereby polystyrene wells were coated with wheat-germ agglutinin, which binds with high affinity to the glycosyl moiety of GC. This strategy left the thrombin-binding domain of GC, which is located a long way from the glycosylated region of the molecule, available for interaction with thrombin [1].

All solid-phase experiments were carried out using 96-well polystyrene trays purchased from Dynatech [Immunlon (high protein-binding capacity)]. Wheat-germ lectin (10 μg/ml) was coated on the wells of a solid-phase plate (150 μl/well) by incubation overnight at 4 °C in 50 mM carbonate buffer, pH 9.50. The blanks were incubated with 1 % BSA (fatty acid-free) in the same buffer. The remaining binding capacity of the sample wells was saturated by a 2 h incubation with 1 % BSA in Hepes-buffered saline, pH 7.5 (10 mM Hepes, 0.15 M NaCl, 0.1 % PEG 6000; buffer A). After aspiration of the BSA solution purified GC was applied to the sample wells at a concentration of 20 μg/ml (150 μl/well) in buffer A and incubated at 4 °C for 1 h. After aspiration, 150 μl of a thrombin solution was applied to each well in duplicate at different concentrations, typically ranging from roughly 0.5 nM to 1 μM in 10 mM Hepes/0.1 M NaCl, pH 7.5. The pH was kept constant at all temperatures studied, by adjusting it at 25 °C to the desired value, using the relation $\Delta pH/\Delta T = -0.014$. Thrombin was incubated for 1 h as preliminary kinetic experiments showed that the reaction reached equilibrium in this time. Each sample and blank well was washed with 250 μl of 0.05 % Tween 20 in buffer A (kept cold to minimize thrombin dissociation) for 10 s. The washing buffer was aspirated and thrombin was detected by incubating each well with 150 μl of 100 μM 52238 in 50 mM Tris, pH 8.0, containing 0.2 M NaCl and 0.1 % PEG 6000, at 25 °C. Colour development at 405 nm is directly proportional to the thrombin bound to immobilized GC. A_{405} was measured using a Sorin-Biomedica (Milan, Italy) ETI-SYSTEM plate reader. A_{405} was found to be linear over 1 h of incubation with substrate, so significant substrate depletion could be excluded. Blanks gave a signal that was about 25 % of that of the corresponding sample. This value was always subtracted from that of the sample. Each determination (sample and blank) was performed in duplicate. The apparent equilibrium dissociation constant, K_d, was calculated using the following relation:

$$\Delta A = \Delta A_{max} \frac{T}{T + K_d} \quad (1)$$

where ΔA is the corrected absorbance value at 405 nm after 1 h of incubation with substrate and T is the thrombin concentration.

Thrombin–GC interaction: effect of heparin, mAbs LJ-Ib10/LJ-Ib1 and F2

The effect of high-molecular mass heparin was evaluated by the solid-phase method. A competitive model was used to analyse the data. Eight curves (96 points) of thrombin binding to immobilized GC, taken at different fixed heparin concentrations, ranging from 0.3 to 20 μM, and over thrombin concentrations spanning 1 nM to 1 μM, were simultaneously fitted to the following equation:

$$\Delta A = \Delta A_{max} \frac{T\alpha}{(T/\alpha) + K_d} \quad (2)$$

where α is equal to $1 + (H/K_i)$, H being heparin concentration and K_i the apparent equilibrium dissociation constant of heparin binding to thrombin.

The effects of mAbs LJ-Ib10 and LJ-Ib1, prothrombin F2 and GC in solution on the binding of 100 nM thrombin to immobilized GC were also studied by the solid-phase method. LJ-Ib10 and LJ-Ib1 were tested at concentrations ranging from 0 to 0.6 mg/ml, and F2 was used over a 0–10 μM concentration range. The effect of GC in solution was evaluated over the concentration range 0–130 nM.

Determination of rate constants for inactivation of thrombin by ATIII in the presence and absence of heparin and GC

Heparin-catalysed inactivation of thrombin by ATIII was demonstrated to proceed via an intermediary thrombin–heparin–ATIII ternary complex, which is predominantly formed by a heparin–ATIII complex reacting with free thrombin [12,13].

On formation of the ternary complex, the adduct rearranges as follows:

$$T + AT\text{–}H \overset{K_{T\text{–}ATH}}{\leftrightarrow} T\text{–}AT\text{–}H \overset{k_{T\text{–}ATH}}{\leftrightarrow} T\text{–}AT + H \quad (3)$$

where T, AT and H represent thrombin, ATIII and heparin respectively, $K_{T\text{–}ATH}$ is the equilibrium constant for thrombin binding to the AT–H complex and $k_{T\text{–}ATH}$ is the rate constant for conversion of the reversible ternary T–AT–H adduct into a stable T–AT complex and free heparin. Inactivation of thrombin can be monitored through competitive chromogenic substrate

hydrolysis. When ATIII is used at concentrations much higher than K_d for high-affinity heparin binding [14], hydrolysis of the *p*-nitroanilide substrate as a function of time can be described by the following equation [15]:

$$[\text{pNA}]_t = [\text{pNA}]_\infty (1 - e^{-k_{obs}t} + bt) \quad (4)$$

where $[\text{pNA}]_t$ and $[\text{pNA}]_\infty$ are the concentrations of released *p*-nitroaniline at time t and ∞ respectively, b is a baseline correction compensating for any non-enzymic substrate cleavage and k_{obs} is an apparent rate constant equal to:

$$k_{obs} = \frac{k_{T-ATH}[\text{AT–H}]}{K_{T-ATH}\{1 + [S]_0/K_m\} + [\text{AT–H}]} \quad (5)$$

where $[S]_0$ is the concentration of the chromogenic substrate, K_m is the Michaelis constant for substrate hydrolysis and [AT–H] is the concentration of the AT–heparin complex.

The pseudo-first-order rate of thrombin inhibition by ATIII in the presence of heparin was determined at 25 °C using 1 nM thrombin, 0.15 μM ATIII and 50 nM high-molecular-mass heparin in 10 mM Hepes/0.15 M NaCl/0.1 % PEG 6000, pH 7.5 (buffer A). Thrombin inactivation was monitored continuously through competitive chromogenic substrate hydrolysis. The concentration of the substrate S2238 was always about 100 μM. The release of *p*-nitroaniline was monitored at 405 nm, using a thermostatically controlled Varian Cary 2200 spectrophotometer. When the effect of GC on thrombin inhibition by the ATIII–heparin complex was tested, GC was incubated at concentrations ranging from 0 to 1.75 μM with ATIII, heparin and S2238, before addition of thrombin. Experimental points were then fitted to eqn. (5).

The kinetic constant pertaining to thrombin inactivation by ATIII in the absence of heparin was measured by the method of Olson et al. [13]. Briefly, reaction of 2 nM thrombin with 1.5 μM ATIII in the presence of 100 μM S2238 was studied in buffer A at 25 °C. The release of *p*-nitroaniline was continuously recorded as described above. Experimental points were fitted to the following relation:

$$[\text{pNA}]_t = [\text{pNA}]_\infty (1 - e^{-k_{obs}t}) \quad (6)$$

where k_{obs} is the rate constant for thrombin inactivation, equal to $[\text{ATIII}]/[1 + (S_0/K_m)]$ times the value of the second-order rate constant of thrombin–ATIII interaction.

Effect of temperature on thrombin–GC interaction

In the temperature experiments, the polystyrene plates for the solid-phase assay were preincubated for 1 h at the desired temperature in a Heto CB 7 water-bath, equipped with a Heto DT622-1 temperature controller. The actual temperature inside the wells was always checked with a microthermometer. The same preincubation procedure was performed for all the reagents used in the solid-phase experiments.

The effect of temperature on thrombin–GC interaction was studied over a 4–37 °C temperature range. The apparent association equilibrium constants, K_a, measured at all temperatures were fitted to the integrated form of the van't Hoff equation:

$$\ln \frac{K_a}{K_a^0} = \frac{\Delta H_0 - T_0 \Delta C_p}{R} \left(\frac{1}{T_0} - \frac{1}{T} \right) + \frac{\Delta C_p}{R} \ln \frac{T}{T_0} \quad (7)$$

where T_0 is an arbitrarily chosen reference temperature expressed in K and K_a^0 and ΔH_0 are temporarily assigned values of the equilibrium association constant and van't Hoff enthalpy at that temperature. The heat capacity change, ΔC_p, was assumed to be independent of temperature. These parameter values were computed by means of a non-linear fitting procedure using SigmaPlot software (Jandel Scientific).

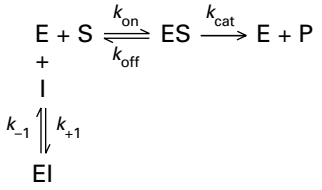

Scheme 1

E is thrombin, S is the chromogenic substrate and I is hirudin.

Effect of GC on thrombin–hirudin interaction

Thrombin–hirudin interaction was studied according to the classical scheme (Scheme 1) describing the competitive effect of hirudin binding on the hydrolysis of a chromogenic peptide by thrombin [16].

Progress curve data, pertaining to thrombin hydrolysis of substrate, were analysed as previously described [16]. Briefly, since in 20 mM Tris/HCl/0.2 M NaCl/0.1 % PEG 6000, pH 7.9, at 25 °C (buffer B) the inhibition by hirudin develops slowly on addition of thrombin, the concentration of hydrolysed substrate, P, at time t is equal to [16,17]:

$$[P]_t = v_\infty t + \frac{(v_i - v_\infty)(1-\gamma)}{\lambda\gamma} \ln \frac{1 - \gamma e^{-\lambda t}}{1-\gamma} \quad (8)$$

where v_i is the initial velocity of the substrate hydrolysis and v_∞ is the steady-state velocity of substrate hydrolysis. The values of K_m and k_{cat} (the Michaelis constants for substrate hydrolysis) were measured in separate experiments, under steady-state conditions and in the absence of hirudin. The relevant expressions for v_i, v_∞, γ and λ are [17]:

$$v_i = e_T \frac{k_{cat} S}{K_m + S} \quad (9a)$$

$$v_\infty = v_i \frac{e_T - H_T - K_i + Q}{2 e_T} \quad (9b)$$

$$\gamma = \frac{e_T + H_T - K_i - Q}{e_T + H_T - K_i + Q} \quad (9c)$$

$$\lambda = \beta Q \quad (9d)$$

$$\beta = k_{+1} \frac{K_m}{K_m + S} \quad (9e)$$

$$K_i = K_i^0 \left(1 + \frac{S}{K_m}\right) \quad (9f)$$

$$Q = \sqrt{[(e_T + H_T + K_i)^2 - 4 e_T H_T]} \quad (9g)$$

where e_T and H_T are total thrombin and hirudin concentrations, respectively. The inhibition constant K_i^0 is equal to the equilibrium dissociation constant of hirudin binding, $K_d = k_{-1}/k_{+1}$.

Typically 0.1 nM thrombin was added to buffer B containing 100 μM S2238 and hirudin (0–250 pM). Ten hirudin concentrations were usually tested and the signal reflecting *p*-nitroaniline hydrolysis by thrombin was followed at 405 nm. All the set data points (132 points) were simultaneously fitted to eqns. (8) and

(9a–g), and the best-fit values of both K_i^0 and k_{+1} were obtained in all cases.

When the effect of GC was tested, the purified glycoprotein was incubated at fixed concentrations ranging from 0 to 0.75 μM with S2238 and hirudin, as described above, and 0.1 nM thrombin was finally added.

RESULTS

Thrombin–GC interaction evaluated by the solid-phase assay

The mAb LJ-Ib10, which selectively inhibits thrombin binding to GpIb [18], was used to demonstrate the specificity of the solid-phase method. This antibody caused a dose-dependent inhibition of thrombin–GC interaction. In contrast, mAb LJ-Ib1, which specifically interacts with the von Willebrand factor-binding domain of GC without perturbing thrombin–GC interaction [18], did not alter thrombin binding to immobilized GC (Figure 1).

Quantitative analysis of thrombin binding to immobilized GC demonstrated that the enzyme binds to a single site on the glycoprotein molecule. *F*-testing showed that the goodness of the fit was not significantly improved by using a two-site Adair equation ($F = 1.029$; $P = 0.979$).

In addition, as clearly shown by Figure 2, high-molecular-mass heparin can displace thrombin from GC immobilized on polystyrene wells. This finding is in agreement with recent results obtained by measuring thrombin binding to GC immobilized on an agarose-affinity matrix [5]. Moreover, the calculated equilibrium dissociation constants of heparin–thrombin and thrombin–GC interactions at 4 °C were in the micromolar and nanomolar range respectively (see the legend to Figure 2), as previously reported [19,20].

Also, prothrombin F2 can displace thrombin from immobilized GC (Figure 3), in agreement with crystallographic studies indicating that prothrombin F2 binds to the heparin-binding domain of thrombin [10].

Finally, it is noteworthy that GC in solution was also able to displace competitively thrombin bound to immobilized GC (Figure 4).

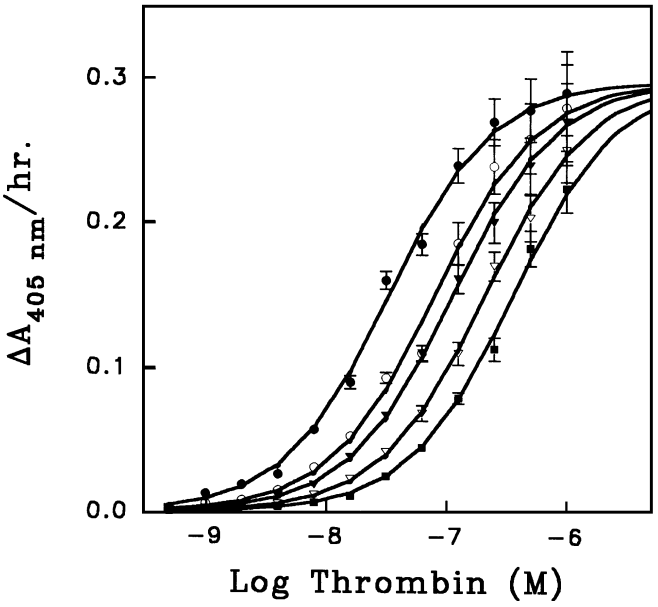

Figure 2 Thrombin binding to immobilized platelet GC in the presence of heparin at 4 °C under the experimental conditions reported in the text

Heparin concentrations were 0 (●), 0.31 (○), 0.62 (▼), 1.25 (▽) and 2.5 (■) μM. For the sake of clarity, only five of eight curves are shown. The lines are drawn according to eqn. (2) with the best-fit parameter values: $\Delta A_{max} = 0.298 \pm 0.07$, $K_d = 29.6 \pm 2.3$ nM and $K_i = 0.23 \pm 0.02$ μM. Vertical bars indicate S.D.s derived from two data sets.

Effect of GC on thrombin–ATIII interaction

In the absence of heparin, GC does not change the kinetics of thrombin interaction with ATIII. The apparent second-order rate constant of thrombin–ATIII interaction was found to be $(1.6 \pm 0.2) \times 10^4$ $M^{-1} \cdot s^{-1}$ and $(1.5 \pm 0.1) \times 10^4$ $M^{-1} \cdot s^{-1}$ in the absence and presence of 1 μM GC respectively.

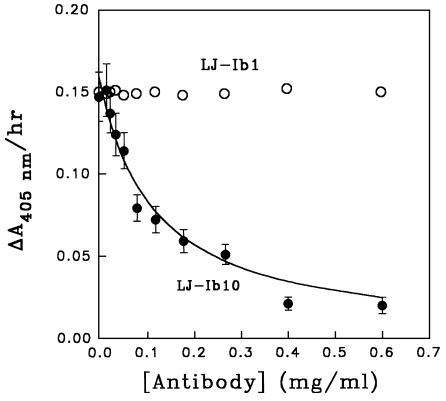

Figure 1 Binding of α-thrombin to immobilized GC at 25 °C under the experimental conditions reported in the text

The effect of mAbs LJ-Ib10 (●) and LJ-Ib1 (○) on the binding of 100 nM α-thrombin are shown. The line is drawn according to a competitive model for LJIb10, giving an apparent IC_{50} value of 0.1 ± 0.001 mg/ml. Vertical bars are S.D.s derived from two different experiments.

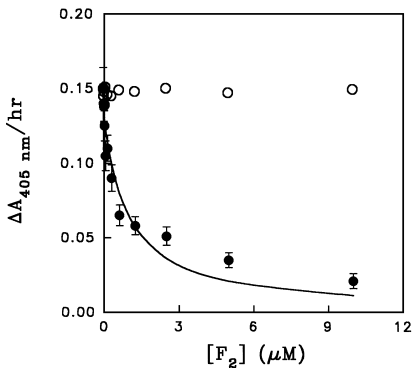

Figure 3 Effect of prothrombin F2 fragment (●) on the binding of 100 nM α-thrombin to immobilized GC at 25 °C under the experimental conditions reported in the text

○, Corresponding blank, where only plain buffer was used. The line is drawn according to a competitive model giving an IC_{50} value of 0.92 ± 0.12 μM. Vertical bars are S.D.s derived from two data sets.

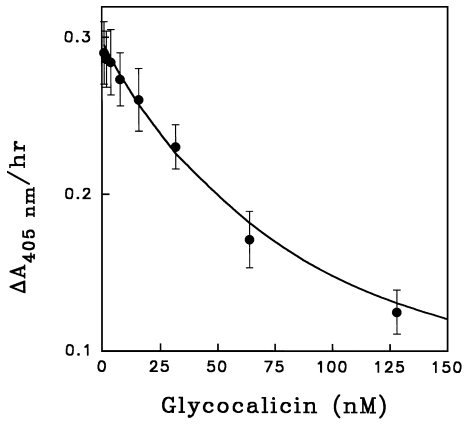

Figure 4 Effect of GC in solution on 100 nM thrombin binding to immobilized GC at 25 °C under the experimental conditions reported in the text

The line was drawn according to a competitive inhibition effect. Vertical bars are S.D.s derived from two data sets.

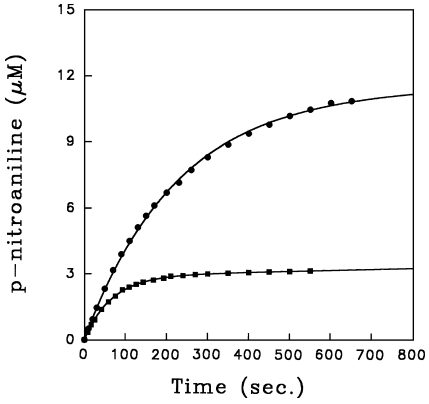

Figure 5 Effect of GC on α-thrombin inhibition by human ATIII in the presence of heparin under the experimental conditions reported in the text

Data points obtained at 0 (■) and 1.75 (●) μM GC are shown. Thrombin, ATIII and heparin concentrations were 1, 150 and 50 nM respectively. The concentration of substrate S2238 was 100 μM. The lines are drawn according to eqn. (4) with the best-fit parameter values: ■, $[pNA]_\infty = 2.9 \pm 0.006$ μM, $k_{obs} = (1.52 \pm 0.013) \times 10^{-2}$ s^{-1}, $b = 0.556 \pm 0.03$ nM/s; ●, $[pNA]_\infty = 11.1 \pm 0.006$ μM, $k_{obs} = (4.56 \pm 0.06) \times 10^{-3}$ s^{-1}, $b = 0.56 \pm 0.05$ nM/s.

In contrast, in the presence of heparin, the apparent rate constant of thrombin–ATIII interaction decreased as a function of GC (Figures 5 and 6). The experimental values for the apparent rate constants for thrombin inactivation by heparin–ATIII measured in the presence of different GC concentrations were fitted to the following phenomenological relation:

$$k_{app} = k_0 + \frac{(k_{min} - k_0)[GC]}{K_d^* + [GC]} \quad (10)$$

where k_0 and k_{min} are the apparent pseudo-first-order rate constants for thrombin inactivation at zero and saturating GC respectively, and K_d^* is an apparent binding constant related to the equilibrium dissociation constant of thrombin–GC interaction. From inspection of eqn. (5), it is evident that the apparent rate constant of thrombin–ATIII–heparin interaction, k_{obs}, is directly proportional to the k_{T-ATH}/K_{T-ATH} value. Thus, if an

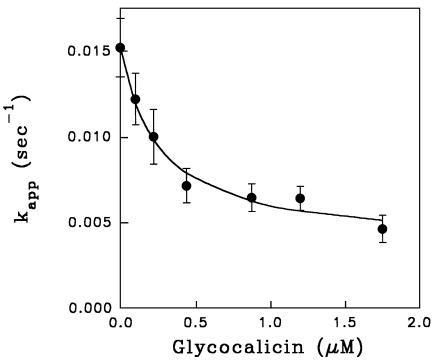

Figure 6 Effect of GC on the apparent kinetic constant of thrombin inhibition by ATIII in the presence of 50 nM heparin

The line is drawn according to eqn. (10) with the best-fit parameter value: $k_0 = (1.53 \pm 0.06) \times 10^{-2}$ s^{-1}, $k_{min} = (3.6 \pm 0.7) \times 10^{-3}$ s^{-1}, $K_i = 250 \pm 70$ nM. Means ± S.D. from two separate experiments are shown.

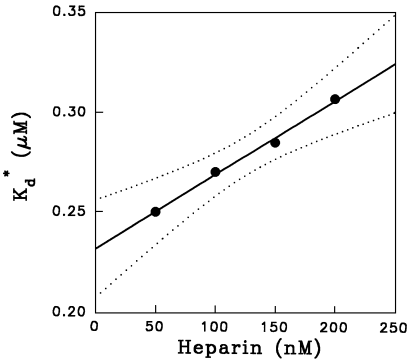

Figure 7 Effect of heparin on the apparent binding constant of thrombin–GC interaction, derived from application of eqn. (10)

The solid line is a linear regression ($r = 0.99$), with the dotted lines representing the 99% confidence limits.

effector molecule does not cause a change in K_m and/or the [AT–H], a reduction in k_{obs} can be attributed to a reduction in the k_{T-ATH}/K_{T-ATH} value.

In separate experiments using a Perkin–Elmer LS5B spectrofluorimeter and the method of Olson and Shore [14], the value of equilibrium binding of high-affinity heparin to ATIII, K_{AT-H}, was found to be 20 ± 4 nM, in good agreement with previously reported values [14]. This value was not significantly changed (25 ± 6 nM) by 1 μM GC, which therefore does not alter [AT–H]. Similarly, the K_m and k_{cat} values from thrombin hydrolysis of the chromogenic substrate S2238 were not found to be changed in the presence of 1.2 μM GC (2.5 ± 0.2 μM and 98 ± 5 s^{-1} and 2.6 ± 0.3 μM and 100 ± 6 s^{-1} respectively). Therefore the reduction in apparent k_{obs} as a function of GC concentration, occurring solely in the presence of heparin, can be attributed to a reduction in k_{T-ATH}/K_{T-ATH}, which is an expression of the specificity constant for thrombin association with the heparin–ATIII complex. This finding is compatible with direct competition between the glycoprotein and the heparin–ATIII complex for binding to thrombin. This conclusion was further validated by the finding that the apparent K_d^* of thrombin–GC interaction increased linearly as a function of heparin concentration, as expected for a competitive inhibitory effect (Figure 7).

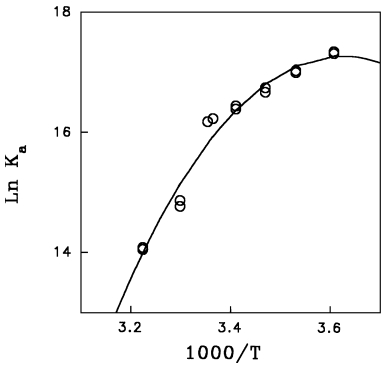

Figure 8 Effect of temperature on the equilibrium association constant of thrombin binding to immobilized GC

The line is drawn according to eqn. (7) with the best-fit parameter values: ΔH° (25 °C) = -11.1 ± 0.7 kcal/mol, $\Delta C_p = -4.14 \pm 0.8$ kJ·mol^{-1}·K^{-1} and K_a° (25 °C) = $(7.4 \pm 0.6) \times 10^6$ M^{-1}.

Table 1 Temperature-dependence of thermodynamic parameters of thrombin–GC interaction calculated using eqn. (7)

The values in parentheses are the experimental ΔG values of binding at that temperature.

Temperature (°C)	ΔG (kcal·mol^{-1})	ΔH (kcal·mol^{-1})	$T\Delta S$ (kcal·mol^{-1})	ΔC_p (kJ·mol^{-1}·K^{-1})
4	-9.51 ± 1.10 (-9.54 ± 0.16)	-0.63 ± 0.15	8.88 ± 3.14	-4.14 ± 0.8
10	-9.60 ± 1.40 (-9.58 ± 0.14)	-3.60 ± 1.01	6.01 ± 2.50	-4.14 ± 0.8
15	-9.62 ± 1.40 (-9.57 ± 0.23)	-6.10 ± 0.60	3.53 ± 0.86	-4.14 ± 0.8
20	-9.54 ± 1.50 (-9.57 ± 0.26)	-8.60 ± 0.50	0.95 ± 0.20	-4.14 ± 0.8
24	-9.41 ± 1.50 (-9.59 ± 0.27)	-10.60 ± 0.60	-1.20 ± 0.30	-4.14 ± 0.8
25	-9.40 ± 1.50 (-9.59 ± 0.25)	-11.10 ± 0.70	-1.71 ± 0.40	-4.14 ± 0.8
30	-9.10 ± 1.50 (-8.93 ± 0.44)	-13.60 ± 1.00	-4.50 ± 1.10	-4.14 ± 0.8
37	-8.62 ± 1.20 (-8.67 ± 0.11)	-17.00 ± 1.60	-8.42 ± 2.00	-4.14 ± 0.8

Effect of temperature on thrombin–GC interaction

The effect of temperature on the equilibrium constant for thrombin–GC interaction can differentiate the free energy of interaction into its enthalpic and entropic factors. As shown in Figure 8, the logarithm of the equilibrium association constant does not correlate linearly with temperature, indicating heat capacity change on formation of the thrombin–GC complex. This phenomenon is generally referred to as a hydrophobic effect [21]. Data on the temperature-dependence of K_a for the thrombin–GC interaction were analysed by using eqn. (7), assuming that ΔC_p is constant over the temperature range studied. All the relevant thermodynamic parameters pertaining to thrombin–GC interaction measured over a 4–37 °C temperature range are listed in Table 1. The large negative ΔC_p dictates the thermodynamics of the thrombin–GC complex-formation, causing the net thermodynamic driving force for association of the reactants to shift from entropic to enthalpic as a function of increasing temperature over the physiological range.

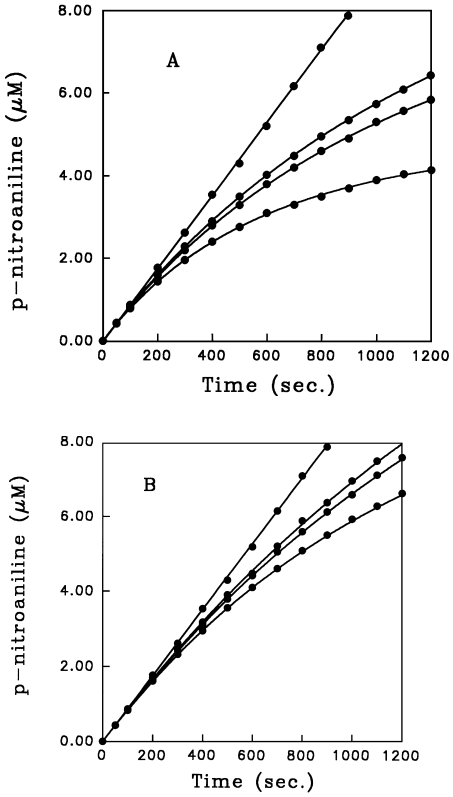

Figure 9 Effect of GC on the thrombin–hirudin interaction under the experimental conditions reported in the text

In (**A**) GC = 0; in (**B**) GC = 750 nM The lines are drawn according to eqns. (8) and (9a–g), with the best-fit parameter values reported in Table 1. For the sake of clarity only four (0, 50, 75 and 200 pM, from top to bottom) of ten curves are shown for each data set. The concentration of thrombin was 100 pM.

Table 2 Kinetic constants for the thrombin–hirudin interaction in the presence of different GC concentrations

Assays were performed and data were analysed as described in the text. The best-fit parameter values are means ± S.E.M. obtained by analysis according to eqns. (8) and (9a–g).

[GC] (μM)	$10^8 \times k_{+1}$ (M^{-1}·s^{-1})	$10^{-4} \times k_{-1}$ (s^{-1})	K_i (pM)
0	3.01 ± 0.02	0.92 ± 0.04	0.31 ± 0.01
0.3	2.40 ± 0.02	1.13 ± 0.06	0.47 ± 0.02
0.5	1.30 ± 0.01	1.25 ± 0.05	0.96 ± 0.03
0.75	1.00 ± 0.02	1.40 ± 0.08	1.40 ± 0.05

Effect of GC on thrombin–hirudin interaction

Application of eqns. (8) and (9a–g) to the experimental data sets on thrombin–hirudin interaction allowed us to differentiate the value of the equilibrium dissociation constant into its association and dissociation rates (Figures 9A and 9B). GC causes a change in both the association and dissociation rate constants of hirudin binding. As listed in Table 2, the value of k_{+1} is reduced about 3-fold, whereas k_{-1} increases about 2-fold over a 0–750 nM GC concentration range. This finding ruled out the possibility of competitive inhibition of GC binding by hirudin, because in that

case only the association rate constant of hirudin binding would be reduced by GC ligation. Moreover this result is in agreement with the hypothesis that the thrombin fibrinogen-recognition site (FRS), which is directly involved in hirudin binding, is not shared by GC. The phenomenological effect of GC binding to thrombin–hirudin interaction is thus linked to allosteric transition of the thrombin molecule.

DISCUSSION

The data reported here show that the solid-phase method is simple, reproducible and accurate, being able to measure an equilibrium dissociation constant in the nanomolar range. The value found for the equilibrium dissociation constant at 20–25 °C is very close to that previously found using radiolabelled α-thrombin and GC immobilized on an agarose-affinity matrix [5,22,23]. Involvement of the thrombin HBS in the GC ligation was demonstrated by using several ligands that interact with that exosite. This evidence confirms previous findings that heparin can competitively displace thrombin from its binding site on the GC molecule [5]. It is known from previous studies that the region of the GC molecule involved in thrombin ligation comprises a large portion of the glycoprotein, particularly residues from Cys-209 to Asp-287 [4,22–24]. It is noteworthy that this region bears an unusual stretch of acidic residues from Asp-269 to Asp-287, comprising three sulphated groups at Tyr-276, Tyr-278 and Tyr-279 [23,25]. It is likely that such a strongly acidic stretch acts as a 'heparin-like' ligand for the thrombin HBS.

The functional consequence of the competitive effect of GC on heparin binding was also evaluated. It was found that GC binding to thrombin protects the enzyme from ATIII inactivation in the presence of heparin. It is thus intriguing to speculate that, besides the effect on platelet activity [26,27], thrombin binding to GpIb is also able to prevent thrombin inactivation by ATIII on the platelet membrane, increasing availability of the enzyme for platelet activation. Moreover, since GpIb binds to the HBS of thrombin, both the catalytic site and the FRS domains of the enzyme remain available for hydrolysis of the thrombin receptor PAR1, a crucial step for full platelet activation [26–30]. Whether the high-affinity thrombin binding to GpIb exerts positive modulatory effects on PAR1 proteolysis remains to be established.

The prothrombin F2, which binds to thrombin HBS [10], also acted as a competitive inhibitor of GC binding to thrombin. On the basis of this evidence and the crystal structure of the thrombin–prothrombin F2 complex [10], it is possible to tentatively map the thrombin domain involved in GpIb ligation. GC interaction with thrombin may share, at least in part, the thrombin area involved in the binding of F2. Many polar interactions have been demonstrated to occur between thrombin and prothrombin F2, although a relevant hydrophobic component enhances the binding strength between these interacting molecules [10]. Several hydrophobic residues in the enzyme molecule, such as Pro-92, Tyr-94, Trp-96 (contained in the so-called 99-loop) and Trp-237, are in fact involved in contacts of less than 0.4 nm (4 Å) with apolar residues of F2 [10] (thrombin amino acid residues numbered according to the chymotrypsin numbering system).

That a hydrophobic component also plays a relevant role in the energetics of thrombin–GC interaction is demonstrated by the temperature-dependence of thrombin binding to GC. This interaction is dominated by a large negative heat capacity change, roughly equal to -4 kJ mol$^{-1}\cdot$K^{-1}. Two factors primarily contribute to the negative heat capacity change observed for processes involving proteins in solution: (a) a change in the vibrational frequency of the proteins; and (b) a change in non-polar surface area exposed to solvent [21]. It was previously found that the ΔC_p value is mainly a function of burial of non-polar surface area on protein–ligand interaction [31,32]. It is thus likely that such biophysical phenomena also accompany the formation of the thrombin–GC adduct.

Together these findings suggest that, as for many protein–protein interactions, the electrostatic bonds between GC and thrombin preorientate these macromolecules so that productive complex-formation is facilitated. The hydrophobic interaction may subsequently strengthen the interaction, leading to the final stable adduct formation.

Finally, the occurrence of allosteric transitions caused in the thrombin molecule by GC binding was demonstrated by the hirudin experiments. The allosteric linkage between GC and hirudin binding to thrombin also rules out direct GC ligation of the thrombin FRS. The data on hirudin agree with previous findings by our laboratory and others that GC binding does not decrease competitively the thrombin specificity for other ligands that bind to the FRS, such as fibrinogen and PAR1 [5,33]. In fact, although GC binding can decrease thrombin affinity for hirudin, this inhibitory effect is caused by a simultaneous decrease in the association rate constant and an increase in the dissociation velocity of the thrombin–hirudin adduct. It is worthy of interest that a similar result was previously found for heparin binding to thrombin [34].

It is not in the realm of this study to elucidate the mechanisms by which this allosteric transition takes place. However, the mutually competitive binding of heparin and GC to thrombin HBS suggests that some thrombin residues such as Arg-93 and Arg-101, which play a critical role in both heparin and F2 interactions [10,35], may also be involved in GC ligation. Such thrombin residues are contained in the thrombin 99-loop, which frames the active-site cleft and is involved in hydrophobic interactions with the N-terminal domain of hirudin [36]. Ligation of Arg-93 and/or Arg-101 may thus affect the conformational state of the 99-loop, perturbing the interactions between thrombin and hirudin, as experimentally demonstrated for both heparin and GC.

This study was financially supported by grant no. 94.02636.CT04, from the National Research Council (CNR) of Italy. The gift of the mAbs LJ-Ib10 and LJ-Ib1 from Dr. L. De Marco is gratefully acknowledged.

REFERENCES

1 Clemetson, K. and Clemetson, J. (1995) Semin. Thromb. Haemost. **21**, 130–137
2 Buchanan, S. ST. C. and Gay, N. J. (1996) Prog. Biophys. Mol. Biol. **65**, 1–44
3 Phillips, D. and Agin, P. (1977) J. Biol. Chem. **252**, 2121–2126
4 Gralnick, J. R., Williams, L. P., McKeown, K., Hansmann, J. W., Fenton, J. W. and Krutzsch, H. (1994) Proc. Natl. Acad. Sci. U.S.A. **91**, 6334–6338
5 De Candia, E., De Cristofaro, R., De Marco, L., Mazzucato, M., Picozzi, M. and Landolfi, R. (1997) Thromb. Haemost. **77**, 735–740
6 De Cristofaro, R., Rocca, B., Bizzi, B. and Landolfi, R. (1993) Biochem. J. **289**, 475–480
7 Nordenman, B. and Björk, I. (1978) Biochemistry **17**, 3339–3344
8 Nordenman, B., Nyström, G. and Björk, I. (1977) Eur. J. Biochem. **78**, 195–203
9 Fox, J. E. B., Aggerbeck, L. P. and Berndt, M. C. (1988) J. Biol. Chem. **263**, 4882–4890
10 Arni, R. K., Padmanabhan, K., Padmanabhan, K. P., Wu, T. P. and Tulinsky, A. (1993) Biochemistry **32**, 4727–4737
11 Pace, C. N., Vaydos, F., Fee, L., Grimsley, G. and Gray, T. (1995) Protein Sci. **4**, 2411–2423
12 Olson, S. T. and Björk, I. (1991) J. Biol. Chem. **266**, 6353–6364
13 Olson, S. T., Björk, I. and Shore, J. (1993) Methods Enzymol. **222**, 525–559
14 Olson, S. T. and Shore, J. D. (1981) J. Biol. Chem. **256**, 11065–11072

15 Hogg, P. J. and Jackson, C. M. (1989) Proc. Natl. Acad. Sci. U.S.A. **86**, 3619–3623
16 Stone, S. R. and Hofsteenge, J. (1986) Biochemistry **25**, 4622–4628
17 Cha, S. (1975) Biochem. Pharmacol. **25**, 2695–2702
18 Handa, M., Titani, K., Holland, L. Z., Roberts, J. R. and Ruggeri, Z. M. (1986) J. Biol. Chem. **261**, 12579–12585
19 Olson, S. T., Halvorson, H. R. and Björk, I. (1991) J. Biol. Chem. **266**, 6342–6352
20 Harmon, J. T. and Jamieson, G. A. (1986) J. Biol. Chem. **261**, 15928–15933
21 Sturtevant, J. M. (1977) Proc. Natl. Acad. Sci. U.S.A. **74**, 2236–2240
22 De Marco, L., Mazzucato, M., Masotti, A. and Ruggeri, Z. M. (1994) J. Biol. Chem. **269**, 6478–6484
23 Marchese, P., Murata, M., Mazzucato, M., Pradella, P., De Marco, L. and Ruggeri, Z. M. (1995) J. Biol. Chem. **270**, 9571–9578
24 Hess, D., Schaller, J., Rickli, E. E. and Clemetson, K. J. (1991) Eur. J. Biochem. **199**, 389–393
25 Dong, J. F., Li, C. Q. and Lopez, J. A. (1994) Biochemistry **33**, 13946–13953
26 Greco, N. J., Tandon, N. N., Jones, G. D., Kornhauser, R., Jackson, B., Yamamoto, N., Tanoue, K. and Jamieson, G. A. (1996) Biochemistry **35**, 906–914
27 Greco, N. J., Jones, G. D., Tandon, N. N., Kornhauser, R., Jackson, B. and Jamieson, G. A. (1996) Biochemistry **35**, 915–921
28 Vu, T. K., Wheaton, V. and Couglin, S. R. (1991) Cell **64**, 1057–1068
29 Connolly, A. J., Ishihara, H., Kahn, M. L., Farese, Jr., R. V. and Coughlin, S. R. (1996) Nature (London) **381**, 516–519
30 Ishihara, H., Connolly, A. J., Zeng, D., Kahn, M. L., Zheng, Y. W., Timmons, C., Tram, T. and Couglin, S. R. (1997) Nature (London) **386**, 502–506
31 Spolar, R. S., Livingstone, J. R. and Record, M. T. (1992) Biochemistry **31**, 3947–3955
32 Murphy, K. P. and Freire, E. (1992) Adv. Protein Chem. **43**, 313–361
33 Bouton, M. C., Jandrot-Perrus, M., Moog, S., Cazanave, J. P. and Guillin, M. C. (1995) Biochem. J. **305**, 635–641
34 Stone, S. R. and Hofsteenge, J. (1987) Eur. J. Biochem. **169**, 373–376
35 Gan, Z. R., Li, Y., Chen, Z., Lewis, S. D. and Shafer, J. A. (1994) J. Biol. Chem. **269**, 1301–1305
36 Rydel, T. J., Ravichandran, K. G., Tulinsky, A., Bode, W., Huber, R., Roitsch, C. and Fenton II, J. W. (1990) Science **249**, 277–280

Received 4 December 1997/9 February 1998; accepted 2 March 1998